QEPAS based ppb-level detection of CO and N_2O using a high power CW DFB-QCL

Yufei Ma,[1,2] Rafał Lewicki,[1,*] Manijeh Razeghi,[3] and Frank K. Tittel[1]

[1]*Department of Electrical and Computer Engineering, Rice University, 6100 Main Street, Houston, Texas 77005, USA*

[2]*National Key Laboratory of Science and Technology on Tunable Laser, Harbin Institute of Technology, Harbin 150001, China*

[3]*Center for Quantum Devices, Department of Electrical Engineering and Computer Science, Northwestern University, Evanston, Illinois 60208, USA*

[*]*Rafal.Lewicki@rice.edu*

Abstract: An ultra-sensitive and selective quartz-enhanced photoacoustic spectroscopy (QEPAS) sensor platform was demonstrated for detection of carbon monoxide (CO) and nitrous oxide (N_2O). This sensor used a state-of-the art 4.61 μm high power, continuous wave (CW), distributed feedback quantum cascade laser (DFB-QCL) operating at 10°C as the excitation source. For the R(6) CO absorption line, located at 2169.2 cm^{-1}, a minimum detection limit (MDL) of 1.5 parts per billion by volume (ppbv) at atmospheric pressure was achieved with a 1 sec acquisition time and the addition of 2.6% water vapor concentration in the analyzed gas mixture. For the N_2O detection, a MDL of 23 ppbv was obtained at an optimum gas pressure of 100 Torr and with the same water vapor content of 2.6%. In both cases the presence of water vapor increases the detected CO and N_2O QEPAS signal levels as a result of enhancing the vibrational-translational relaxation rate of both target gases. Allan deviation analyses were performed to investigate the long term performance of the CO and N_2O QEPAS sensor systems. For the optimum data acquisition time of 500 sec a MDL of 340 pptv and 4 ppbv was obtained for CO and N_2O detection, respectively. To demonstrate reliable and robust operation of the QEPAS sensor a continuous monitoring of atmospheric CO and N_2O concentration levels for a period of 5 hours were performed.

OCIS codes: (280.3420) Laser sensors; (140.5965) Semiconductor lasers, quantum cascade; (300.6340) Spectroscopy, infrared; (110.5125) Photoacoustics.

References and links

1. M. A. K. Khalil and R. A. Rasmussen, "Carbon monoxide in the earth's atmosphere: increasing trend," Science **224**(4644), 54–56 (1984).
2. J. A. Logan, M. J. Prather, S. C. Wofsy, and M. B. McElroy, "Tropospheric chemistry: a global perspective," J. Geophys. Res. **86**(C8), 7210–7254 (1981).
3. A. R. Ravishankara, J. S. Daniel, and R. W. Portmann, "Nitrous oxide (N_2O): the dominant ozone-depleting substance emitted in the 21st century," Science **326**(5949), 123–125 (2009).
4. T. Mitsui, M. Miyamura, A. Matsunami, K. Kitagawa, and N. Arai, "Measuring nitrous oxide in exhaled air by gas chromatography and infrared photoacoustic spectrometry," Clin. Chem. **43**(10), 1993–1995 (1997).
5. L. Tao, K. Sun, D. J. Miller, M. A. Khan, and M. A. Zondlo, "Optimization for simultaneous detection of atmospheric N_2O and CO with a quantum cascade laser," in *Conference on Lasers and Electro-Optics*, Technical Digest (CD) (Optical Society of America, 2012), paper ATh3L.
6. J. Li, U. Parchatka, R. Königstedt, and H. Fischer, "Real-time measurements of atmospheric CO using a continuous-wave room temperature quantum cascade laser based spectrometer," Opt. Express **20**(7), 7590–7601 (2012).
7. T. Yuanyuan, L. Wenqing, K. Ruifeng, L. Jianguo, H. Yabai, Z. Yujun, X. Zhenyu, R. Jun, and G. Hui, "Measurements of NO and CO in Shanghai urban atmosphere by using quantum cascade lasers," Opt. Express **19**(21), 20224–20232 (2011).

#179896 - $15.00 USD Received 13 Nov 2012; revised 29 Dec 2012; accepted 29 Dec 2012; published 9 Jan 2013

8. J. Vanderover, W. Wang, and M. A. Oehlschlaeger, "A carbon monoxide and thermometry sensor based on mid-IR quantum-cascade laser wavelength-modulation absorption spectroscopy," Appl. Phys. B **103**(4), 959–966 (2011).
9. B. W. M. Moeskops, H. Naus, S. M. Cristescu, and F. J. M. Harren, "Quantum cascade laser-based carbon monoxide detection on a second time scale from human breath," Appl. Phys. B **82**(4), 649–654 (2006).
10. L. Joly, T. Decarpenterie, N. Dumelié, X. Thomas, I. Mappe-Fogaing, D. Mammez, R. Vallon, G. Durry, B. Parvitte, M. Carras, X. Marcadet, and V. Zéninari, "Development of a versatile atmospheric N_2O sensor based on quantum cascade laser technology at 4.5 μm," Appl. Phys. B **103**(3), 717–723 (2011).
11. D. D. Nelson, B. McManus, S. Urbanski, S. Herndon, and M. S. Zahniser, "High precision measurements of atmospheric nitrous oxide and methane using thermoelectrically cooled mid-infrared quantum cascade lasers and detectors," Spectrochim. Acta A Mol. Biomol. Spectrosc. **60**(14), 3325–3335 (2004).
12. J. B. McManus, M. S. Zahniser, and D. D. Nelson, "Dual quantum cascade laser trace gas instrument with astigmatic Herriott cell at high pass number," Appl. Opt. **50**(4), A74–A85 (2011).
13. J. Mohn, B. Tuzson, A. Manninen, N. Yoshida, S. Toyoda, W. A. Brand, and L. Emmenegger, "Site selective real-time measurements of atmospheric N_2O isotopomers by laser spectroscopy," Atmos. Meas. Tech. Discuss. **5**(1), 813–838 (2012).
14. C. Grinde, A. Sanginario, P. A. Ohlckers, G. U. Jensen, and M. M. Mielnik, "Two clover-shaped piezoresistive silicon microphones for photo acoustic gas sensors," J. Micromech. Microeng. **20**(4), 045010 (2010).
15. A. Elia, F. Rizzi, C. Di Franco, P. M. Lugarà, and G. Scamarcio, "Quantum cascade laser-based photoacoustic spectroscopy of volatile chemicals: application to hexamethyldisilazane," Spectrochim. Acta A Mol. Biomol. Spectrosc. **64**(2), 426–429 (2006).
16. A. A. Kosterev, Y. A. Bakhirkin, R. F. Curl, and F. K. Tittel, "Quartz-enhanced photoacoustic spectroscopy," Opt. Lett. **27**(21), 1902–1904 (2002).
17. L. Dong, A. A. Kosterev, D. Thomazy, and F. K. Tittel, "QEPAS spectrophones: design, optimization, and performance," Appl. Phys. B **100**(3), 627–635 (2010).
18. R. Lewicki, G. Wysocki, A. A. Kosterev, and F. K. Tittel, "QEPAS based detection of broadband absorbing molecules using a widely tunable, cw quantum cascade laser at 8.4 mum," Opt. Express **15**(12), 7357–7366 (2007).
19. C. Bauer, U. Willer, R. Lewicki, A. Pohlkötter, A. Kosterev, D. Kosynkin, F. K. Tittel, and W. Schade, "A Mid-infrared QEPAS sensor device for TATP detection," J. Phys.: Conf. Ser. **157**(1), 012002 (2009).
20. A. A. Kosterev, L. Dong, D. Thomazy, F. K. Tittel, and S. Overby, "QEPAS for chemical analysis of multi-component gas mixtures," Appl. Phys. B **101**(3), 649–659 (2010).
21. H. Yi, K. Liu, W. Chen, T. Tan, L. Wang, and X. Gao, "Application of a broadband blue laser diode to trace NO_2 detection using off-beam quartz-enhanced photoacoustic spectroscopy," Opt. Lett. **36**(4), 481–483 (2011).
22. R. Lewicki, J. Waclawek, M. Jahjah, Y. Ma, E. Chrysostom, B. Lendl, and F. K. Tittel, "A sensitive CW DFB quantum cascade laser based QEPAS sensor for detection of SO_2," in *Conference on Lasers and Electro-Optics*, Technical Digest (CD) (Optical Society of America, 2012), paper ATh5A.
23. S. Gray, A. Liu, F. Xie, and C. E. Zah, "Detection of nitric oxide in air with a 5.2 μm distributed-feedback quantum cascade laser using quartz-enhanced photoacoustic spectroscopy," Opt. Express **18**(22), 23353–23357 (2010).
24. M. Razeghi, "High-performance InP-based Mid-IR quantum cascade lasers," IEEE J. Sel. Top. Quantum Electron. **15**(3), 941–951 (2009).
25. Q. Y. Lu, Y. Bai, N. Bandyopadhyay, S. Slivken, and M. Razeghi, "Room-temperature continuous wave operation of distributed feedback quantum cascade lasers with watt-level power output," Appl. Phys. Lett. **97**(23), 231119 (2010).
26. S. Schilt, L. Thévenaz, and P. Robert, "Wavelength modulation spectroscopy: combined frequency and intensity laser modulation," Appl. Opt. **42**(33), 6728–6738 (2003).
27. X. Chao, J. B. Jeffries, and R. K. Hanson, "Wavelength-modulation-spectroscopy for real-time, in situ NO detection in combustion gases with a 5.2 μm quantum-cascade laser," Appl. Phys. B **106**(4), 987–997 (2012).
28. L. Dong, R. Lewicki, K. Liu, P. R. Buerki, M. J. Weida, and F. K. Tittel, "Ultra-sensitive carbon monoxide detection by using EC-QCL based quartz-enhanced photoacoustic spectroscopy," Appl. Phys. B **107**(2), 275–283 (2012).
29. L. S. Rothman, I. E. Gordon, A. Barbe, D. C. Benner, P. F. Bernath, M. Birk, V. Boudon, L. R. Brown, A. Campargue, J. P. Champion, K. Chance, L. H. Coudert, V. Dana, V. M. Devi, S. Fally, J.-M. Flaud, R. R. Gamache, A. Goldman, D. Jacquemart, I. Kleiner, N. Lacome, W. J. Lafferty, J.-Y. Mandin, S. T. Massie, S. N. Mikhailenko, C. E. Miller, N. Moazzen-Ahmadi, O. V. Naumenko, A. V. Nikitin, J. Orphal, V. I. Perevalov, A. Perrin, A. Predoi-Cross, C. P. Rinsland, M. Rotger, M. Šimečková, M. A. H. Smith, K. Sung, S. A. Tashkun, J. Tennyson, R. A. Toth, A. C. Vandaele, and J. Vander Auwera, "The HITRAN 2008 molecular spectroscopic database," J. Quant. Spectrosc. Radiat. Transf. **110**(9-10), 533–572 (2009).
30. J. B. McManus, M. S. Zahniser, D. D. Nelson, J. H. Shorter, S. Herndon, and E. Wood, "Application of quantum cascade lasers to high-precision atmospheric trace gas measurements," Opt. Eng. **49**(11), 111124 (2010).
31. R. F. Curl, F. Capasso, C. Gmachl, A. A. Kosterev, B. McManus, R. Lewicki, M. Pusharsky, G. Wysocki, and F. K. Tittel, "Quantum cascade lasers in chemical physics," Chem. Phys. Lett. **487**(1-3), 1–18 (2010).

#179896 - $15.00 USD Received 13 Nov 2012; revised 29 Dec 2012; accepted 29 Dec 2012; published 9 Jan 2013

32. R. Lewicki, L. Dong, Y. Ma, and F. K. Tittel, "A compact CW quantum cascade laser based QEPAS sensor for sensitive detection of nitric oxide," in *Conference on Lasers and Electro-Optics*, Technical Digest (CD) (Optical Society of America, 2012), paper CW3B.4.

1. Introduction

Carbon monoxide (CO), one of the major air pollutants globally, is mainly produced and released into the atmosphere by a variety of incomplete combustion activities, including the burning of natural gas, fossil fuel, and other carbon containing fuels. CO has an important impact on atmospheric chemistry through its reaction with hydroxyl (OH) for troposphere ozone formation and also can affect the concentration level of greenhouse gases (e.g. CH_4) [1,2]. Furthermore, CO even at low concentration levels is dangerous to human life and therefore must be accurately and precisely monitored in real time. Nitrous oxide (N_2O) on the other hand is one of the most anthropogenic important greenhouse gases which has a global warming potential of ~280 times greater than carbon dioxide (CO_2), and is the single most important contributor to ozone depletion in the atmosphere [3]. N_2O is mainly produced by human related sources such as agricultural soil management, nitric acid production, as well as combustion of fossil fuels by automobile, truck, and aircraft emissions. It can be also produced naturally from a wide variety of biological sources present in soil and water [4].

Atmospheric detection of CO and N_2O concentration levels using laser absorption spectroscopy based optical gas sensor platforms have been reported by numerous research groups in recent years [5–13]. Direct laser absorption technique employing a multi-pass cell (MPC), where effective optical path length is extended to tens or even to hundreds of meters, typically allows to reach a detection limit of the analyte species at ppm or ppb levels [5–13]. However for ultra-high sensitive measurements these types of sensors are usually bulky due to the large size of a MPC and the increased number of optical components that are needed for laser beam alignment. Another useful technique for trace gas analysis is conventional photo-acoustic spectroscopy (PAS) that employs a broadband microphone for acoustic wave detection. However, most of conventional microphone-based photo-acoustic cells have a resonance at low frequency values (<2 kHz), which makes them more sensitive to environmental and sample gas flow noise. Moreover, the size of the typical photo-acoustic cell is still considered to be large [14,15]. A recent modification of the conventional PAS is the quartz-enhanced photoacoustic spectroscopy (QEPAS) technique that was first reported in 2002 [16]. This technique uses a commercially available mm sized piezoelectric quartz tuning fork (QTF) as an acoustic wave transducer. A high Q-factor and a ~32.7 kHz resonance frequency of the QTF improve QEPAS selectivity and immunity to environmental acoustic noise. Moreover, QEPAS possesses a large dynamic range of nine orders of magnitude of the acoustic signal, a wide temperature range (of up to 700 K), and its noise is limited by the fundamental Johnson thermal noise of the QTF. A significant enhancement of the QEPAS signal can be achieved when two metallic tubes acting as a micro-resonator (mR) are added to the QTF sensor architecture. A recent optimization study of the geometrical mR parameters showed that the highest QEPAS signal-to-noise ratio (SNR) is achieved for two 4.4 mm-long and 0.5-0.6 mm inner diameter tubes [17]. However, for a typical collimated QCL beam diameter between 3 and 5 mm, short mR tubes with a larger inner diameter are advantageous in facilitating the optical alignment of the QCL excitation beam with the respect to the mR and the QTF. Therefore for the DFB-QCL based CO and N_2O QEPAS measurements the length and inner diameter of the mR tubes were selected to be 3.9 mm and 0.84 mm, respectively. For a mR enhanced QTF the total volume of the QEPAS acoustic detection module (ADM) is ~3.8 cm^3 and can be further reduced because the volume of the analyzed gas sample is limited by the dimensions of the QTF and the acoustic mR tubes to ~3 mm^3. Therefore the overall size of a typical QEPAS sensor platform can be significantly reduces to a size that make this device suitable for applications requiring lightweight and compact sensors such as balloon based atmospheric measurements or portable low cost sensors for first

#179896 - $15.00 USD Received 13 Nov 2012; revised 29 Dec 2012; accepted 29 Dec 2012; published 9 Jan 2013

responders, such as in mining accidents or forest fires near urban centers. Like conventional photoacoustic spectroscopy, QEPAS does not require optical detectors. With little or no modification to the spectrophone, this technique can be used in different spectral regions to detect broadband absorbing molecules [18,19], as well as small molecules with narrow linewidth [20]. This feature is especially attractive for gas sensing in the 5-20 μm region, where the availability of high-performance optical detectors is limited, and cryogenic cooling is often required. The QEPAS technique also benefits from the high optical power of QCLs in order to achieve minimum detectable concentration at the ppb or sub-ppb level.

Due to above mentioned advantages the QEPAS technique has been successfully used by several groups as a compact sensor for sensitive detection of various trace gases during the past decade [21–23]. In this manuscript the performance of a state-of the art high power 4.61 μm CW TEC DFB-QCL in combination with ultra-compact and highly sensitive QEPAS sensor technology was demonstrated for the first time.

2. Description of experimental system

2.1 Experimental configuration of QEPAS sensor system

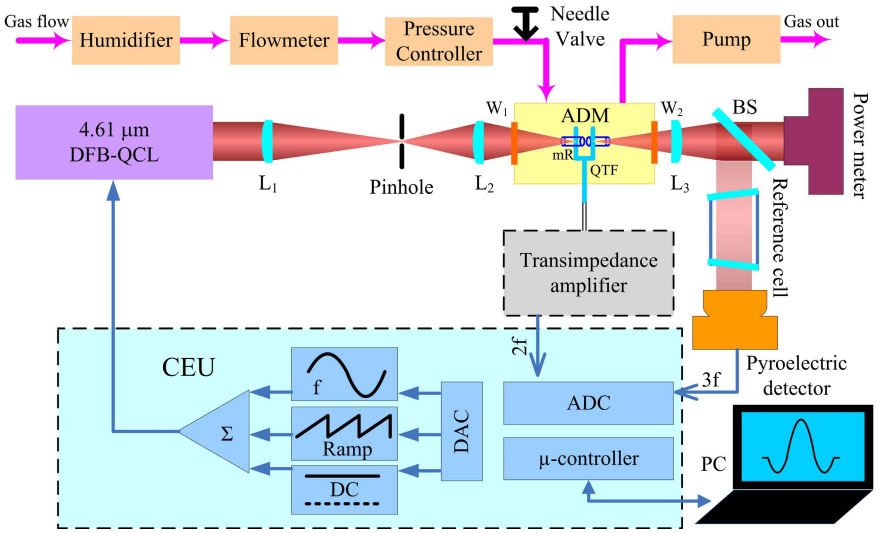

Fig. 1. Schematic configuration of a high power 4.61 μm CW RT TEC DFB-QCL based QEPAS system for ppb detection of CO and N_2O.

A schematic of the QEPAS based CO and N_2O sensor platform is shown in Fig. 1. As an excitation source a 4.61 μm high power, continuous wave (CW), distributed feedback quantum cascade laser (DFB-QCL) operating at 10°C from Northwestern University was employed [24,25]. A compact external water cooling system was used (e.g. the "Oasis" model water chiller available from Solid State Cooling Systems, Inc) to remove the heat dissipation from the hot surface of a TEC mounted in a commercial QCL housing (ILX Lightwave Model LDM-4872). The DFB-QCL beam is collimated using a black diamond antireflection coated (3-5 μm) aspheric lens with a 1.7 mm effective focal length (Lightpath model 390037-IR3). In order to further improve the QCL beam quality two additional 50 mm and 40 mm focal length plano-convex CaF_2 lenses, L_1 and L_2, and a pinhole with diameter of 200 μm as a spatial filter were used. The second lens L_2 was used to direct the laser beam through the mR and the gap between prongs of the QTF, located inside an ADM, with a transmission efficiency of >93%. A ZnSe wedged window acting as a beam splitter (BS) is placed after the ADM to reflect ~20% of the DFB-QCL beam into a gas reference channel. The rest of the high power CW DFB-QCL beam is delivered to an optical power meter (Ophir model 3A-

#179896 - $15.00 USD Received 13 Nov 2012; revised 29 Dec 2012; accepted 29 Dec 2012; published 9 Jan 2013

SH) and used for alignment verification of the QEPAS system. In a reference channel the laser beam, after passing through a reference cell, is detected by a pyroelectric detector (InfraTec model LIE-332f-63). A 3f reference channel signal is employed for locking of the QCL laser frequency to the peak of absorption line of the target analyte. For precise and accurate CO concentration measurements, a 5 cm long reference cell filled with a 500 ppm CO:N_2 mixture at 150 Torr pressure (fabricated by Wavelength References, Inc) was used. For N_2O detection a 10 cm long reference cell filled with 2% N_2O in N_2 at a pressure of 100 Torr was employed. The major reason as to why both reference cells were placed behind the ADM was to minimize any optical power losses between the QCL and the ADM.

To improve the CO and N_2O vibrational-translational relaxation processes an external humidifier was added at the inlet to the QEPAS system. In this case the addition of a 2.6% H_2O vapor concentration to the target trace gas mixture facilitates the slow relaxation processes of both molecules, which do not have a dense ladder of energy levels to lead to sufficiently fast intrinsic V-T relaxation. The presence of H_2O vapor in the analyzed gas increases the V-T relaxation process, which results in a higher detected amplitude for the CO and N_2O QEPAS signals. A needle valve and flow meter (Brandt Instruments, Inc., Type 520) were used to set and monitor the gas flow through the QEPAS sensor system at a constant rate of 140 ml/min. A pressure controller (MKS Instruments, Inc., Type 649) and a vacuum pump were employed to control and maintain the pressure in the system. The DFB-QCL current and temperature were set and controlled by an ILX Lightwave current source (model LDX 3220) and a Wavelength Electronics temperature controller (model MPT10000), respectively.

For sensitive CO and N_2O concentration measurements a wavelength modulation spectroscopy (WMS) with 2nd harmonic detection [26,27] was utilized. Modulation of the laser current was performed by applying a sinusoidal dither to the direct current ramp of the DFB-QCL at half of the QTF resonance frequency ($f = f_0/2$ ~16.3 kHz). The piezoelectric signal generated by the QTF was detected by a low noise transimpedance amplifier with a 10 MΩ feedback resistor and converted into a voltage. Subsequently this voltage was transferred to a custom built control electronics unit (CEU). The CEU provides the following three functions: 1) measurement of the QTF parameters, i.e., the quality factor Q, dynamic resistance R, and resonant frequency f_0; 2) modulation of the laser current at the frequency $f = f_0/2$; and 3) measurement of the $2f$ component generated by the QTF and $3f$ component when the CEU is equipped with an internal reference cell and photodetector.

The optical power emitted by the DFB-QCL operating at 1250 mA current and 10°C temperature is 987 mW in the CW operating mode (see Fig. 2(a)). The experimentally

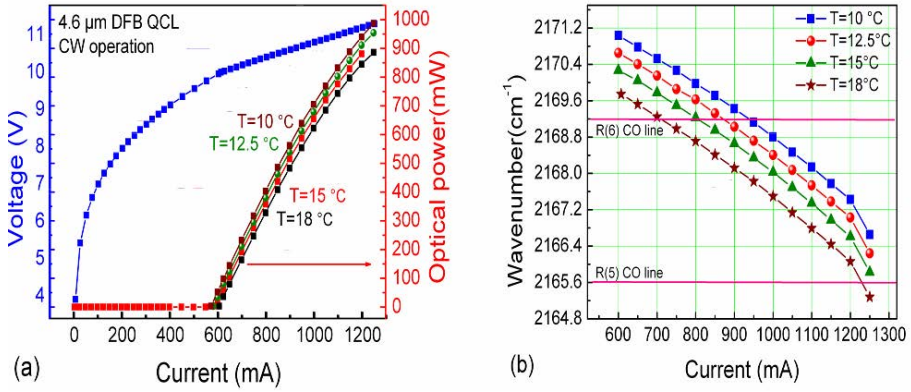

Fig. 2. (a) LIV curve of the 4.61 µm RT, CW, DFB-QCL from center for quantum devices, Northwestern University; (b) DFB-QCL current tuning at different DFB-QCL operating temperatures.

#179896 - $15.00 USD Received 13 Nov 2012; revised 29 Dec 2012; accepted 29 Dec 2012; published 9 Jan 2013

determined temperature and current tuning coefficients are –0.16 cm^{-1}/°C and –0.0065 cm^{-1}/mA, respectively. This DFB-QCL can be current tuned to target the R(5) and R(6) absorption lines of the ν_1 CO fundamental band at 2165.6 cm^{-1} and 2169.2 cm^{-1}, respectively (see Fig. 2(b)).

2.2 Selection of CO and N_2O spectrum absorption line

Quantitative measurements of carbon monoxide in the ν_1 CO fundamental rotational-vibrational band were reported previously by many research groups [5–9, 28]. In Ref. [28] CO detection was performed using the R(8) CO absorption line located at 2176.3 cm^{-1} by employing a Daylight Solutions, Inc external cavity quantum cascade laser (EC-QCL) based QEPAS sensor system. This CO sensor was operating at a reduced gas pressure of 100 Torr in order to avoid partial overlap with neighboring nitrous oxide (N_2O) line. In Ref. [6] the authors targeted the R(12) CO absorption line located at 2190.0 cm^{-1} which has a small spectral overlap with N_2O. However the R(12) line does not have a high absorption line strength compared to other CO lines of the R branch [29]. In this work the R(6) CO absorption line located at 2169.2 cm^{-1} was selected in order to measure the CO concentration with high accuracy and detection sensitivity. To assess potential interferences from other atmospheric species, HITRAN based spectra of CO, N_2O, and H_2O absorption lines near 2169 cm^{-1} were simulated at atmospheric pressure (760 Torr) and depicted in Fig. 3(a). From simulated 2nd harmonic absorption spectra (Fig. 3(b)) it is clear that the R(6) CO line is free from spectral interference and can be measured using wavelength modulation spectroscopy. Furthermore, the R(6) is one of the strongest line in the CO v_1 vibrational band with a 1.54 times higher absorption line strength than the R(12) line. For nitrous oxide concentration measurements, an interference-free P(41) N_2O absorption line located at 2169.6 cm^{-1} was selected at a gas pressure of 100 Torr. For the CW DFB-QCL operating at 10°C the optical power measured after the ADM was 400 mW near 2169 cm^{-1} due to optical power losses by the sensor components (i.e., spatial filter, ADM windows, QTF and the two micro-resonator tubes). High optical power helps to improve QEPAS signal that is proportional to: S_0

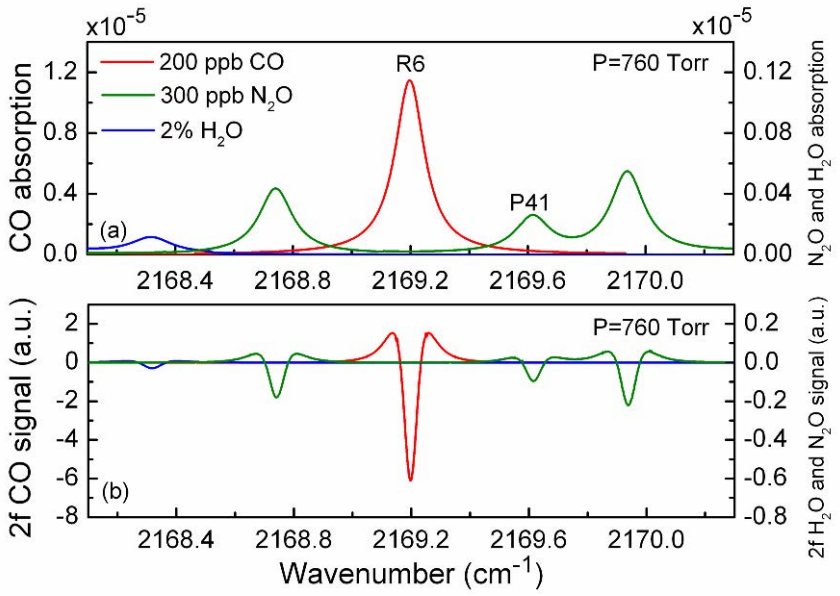

Fig. 3. HITRAN based simulation spectra of CO and N_2O at a temperature of 296 K, a standard atmospheric pressure, an optical path length of 1 cm for 200 ppb CO, 2% H_2O and 300 ppb N_2O, respectively. (a) Absorption spectra; (b) 2nd harmonic absorption spectra.

#179896 - $15.00 USD Received 13 Nov 2012; revised 29 Dec 2012; accepted 29 Dec 2012; published 9 Jan 2013

~($\alpha \cdot P \cdot Q$)/f_0 where α is the absorption coefficient, P is the optical power, Q is the quality factor of the resonator and f_0 is the resonant frequency.

3. Experimental results and discussion

The QEPAS based sensor performance was tested in two operational modes. In the scanning mode, a small amplitude modulation signal at $f_o/2$ frequency was embedded on top of the slowly changing DC current ramp and added to the DC DFB-QCL current offset resulting in mode-hop-free frequency tuning over the targeted absorption line. In the line locking mode, the DFB-QCL frequency was set to the center of the absorption line and actively controlled by the feedback signal of the internal CEU proportional controller based on the 3f component from the pyroelectric detector output (see Fig. 1). The proportional controller signal compensates any laser frequency drift by generating a correction signal to maintain the frequency always at the center of the targeted absorption line.

3.1 Line scanning to detect CO and N_2O concentration levels

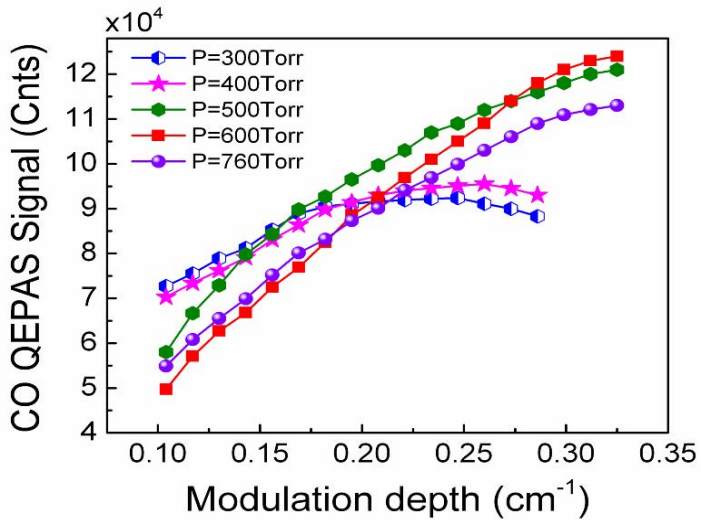

Fig. 4. Measured CO QEPAS signal amplitude as a function of laser modulation depth for a dry 5 ppm CO:N_2 mixture at five different pressure values. The QEPAS signal is recorded in terms of internal CEU units, where 1cnt = 6.67×10^{-16} A.

In order to obtain the maximum 2f QEPAS signal, both the gas pressure and laser wavelength modulation depth must be chosen appropriately. For the purpose of determining the best operating conditions for the CO sensor a certified mixture of 5 ppmv CO in nitrogen (N_2) was used. The results shown in Fig. 4 illustrate the influence of the laser modulation depth and pressure on the QEPAS signal measured at the peak of the R(6) CO absorption line. For the currently used configuration of the ADM the maximum CO QEPAS signal level is obtained at 600 Torr and a modulation depth of 0.325 cm^{-1}. A similar set of measurements was performed for a mixture of 5 ppm CO:N_2 with 2.6% water and no noticeable difference in the curve shape depicted in Fig. 4 was observed. For the same modulation depth the QEPAS signal value at the pressure of 760 Torr is only ~10% lower compared with the maximum CO signal. From a practical point of view it is more convenient to operate the QEPAS sensor at atmospheric pressure, because in this case the pressure controller and flow meter become redundant. For this reason, further evaluation tests of the QEPAS based CO sensor was performed at atmospheric pressure. However to avoid an increase of the QEPAS noise level due to the QTF excitation the flow rate through the sensor system must be kept at a level of

#179896 - $15.00 USD Received 13 Nov 2012; revised 29 Dec 2012; accepted 29 Dec 2012; published 9 Jan 2013

<300 ml/min. To monitor and verify the flow rate in the system an external flow meter was occasionally used in combination with a needle valve.

The QEPAS signal amplitude for a slowly relaxing molecule such as CO is strongly dependent on the V-T (vibrational-translational) relaxation rate. Hence the addition of water vapor to the analyzed gas mixture helps to efficiently improve the energy transfer for the V-T states of the excited CO molecules. Therefore, water vapor at different concentration levels was added into the CO:N_2 gas mixture by means of a commercial permeation tube (Perma Pure model MH-110-24F-4), which was immersed inside a water circulating bath (LAUDA-Brinkmann, LP., RM6). The dependence of the QEPAS signal as a function of the H_2O concentration is shown in Fig. 5. The addition of 2.6% H_2O results in an 8 times improvement of the signal amplitude compared with a dry CO:N_2 gas mixture. The insert (a) to Fig. 5 shows a difference between the WMS 2*f* signals for a dry and moisturized (after the addition of 2.6% H_2O concentration) 5 ppmv CO:N_2 mixture. The insert (b) to Fig. 5 depicts the background signal measured when the ADM was flushed with ultra high purity N_2. This background signal is primarily determined by fundamental thermal noise of the QTF and is not affected by any optical noise related to the laser beam passing through the ADM. Based on the data depicted in Fig. 5 a 1σ minimum detectable concentration limit (MDL) of the DFB-QCL based QEPAS CO sensor is 1.5 ppbv for a 1 sec data acquisition time. The corresponding normalized noise equivalent absorption (NNEA) coefficient is 1.61×10^{-8} $cm^{-1}W/\sqrt{Hz}$. The NNEA coefficient was calculated from the following equation: $NNEA = (\alpha_{min} \cdot P \cdot Q)/\sqrt{\Delta f}$, where α_{min} is the minimum detectable absorption coefficient for SNR = 1, *P* is the optical power, and $\sqrt{\Delta f}$ is the detection bandwidth.

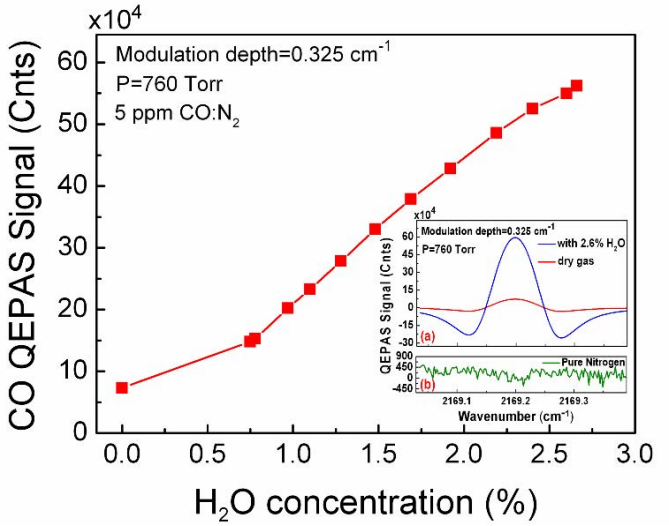

Fig. 5. Measured QEPAS based CO signal amplitude as a function of water vapor concentration at atmospheric pressure and a modulation depth of 0.325 cm^{-1}. 1cnt = 6.67×10^{-16} A. Insert for (a) QEPAS signal for a 5 ppmv CO:N_2 mixture; dry and moisturized with 2.6% H_2O concentration; (b) pure N_2

QEPAS based CO signals in the laboratory air containing 1.6% and 2.6% H_2O concentrations were measured at atmospheric pressure and depicted in Fig. 6, respectively. This range for H_2O concentration was chosen due to a limited capacity of the used silicone hollow fiber membrane module for the air/gas humidification system. However, due to atmospheric conditions, such as temperature, relative humidity, and pressure a water condensation inside the sensor system tubes can occur. Water condensation can be avoided by heating all tubing and the ADM module above the dew point temperature. The laboratory air

#179896 - $15.00 USD Received 13 Nov 2012; revised 29 Dec 2012; accepted 29 Dec 2012; published 9 Jan 2013

1σ CO concentration level for a 1 sec data acquisition time was calculated to be 120 ppbv when the QEPAS based sensor was operated in the scanning mode. This required a normalization of the amplitude of the 2.6% H_2O containing air sample to the amplitude of the 5 ppmv CO:N_2 with the same H_2O content. For the R(6) CO detection at atmospheric pressure no spectral interferences from atmospheric N_2O or H_2O were observed.

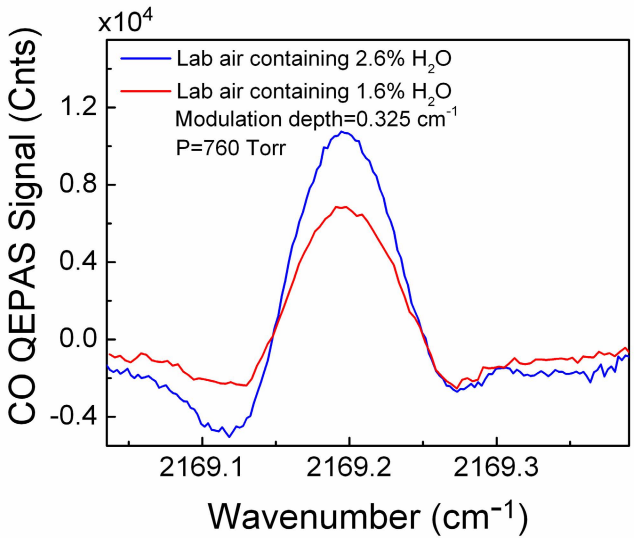

Fig. 6. QEPAS based CO signals for laboratory air containing 1.6% and 2.6% water vapor concentration levels at atmospheric pressure using a DFB-QCL modulation depth of 0.325 cm^{-1}.

Similar measurements were carried out for N_2O detection by targeting the P(41) N_2O absorption line. A certified mixture of 1.8 ppmv N_2O:N_2 was used to evaluate the QEPAS sensor performance in this case. The optimum signal level was obtained when the gas pressure and modulation depth were set to 100 Torr and 0.13 cm^{-1}, respectively. The addition of a 2.6% H_2O concentration to the analyzed N_2O:N_2 mixture resulted in a 5 fold enhancement of QEPAS signal amplitude, which resulted in a MDL of 23 ppbv. The corresponding NNEA coefficient was found to be 2.91×10^{-9} $cm^{-1}W/\sqrt{Hz}$. The N_2O concentration level in laboratory was measured to be 350 ppbv when the QEPAS sensor was operated in the scanning mode.

3.2 Line locking for continuous monitoring of CO and N_2O concentration levels

Continuous monitoring of CO and N_2O concentration levels and the evaluation of the long term sensor performance of the QEPAS based sensor system was performed in the line locking mode, where the CW DFB-QCL frequency is kept at the center of the targeted absorption line. For line-locked measurements of the CO concentration at atmospheric pressure the modulation depth was decreased from 0.325 cm^{-1} to 0.26 cm^{-1} because the 3f reference signal shape for the QEPAS sensor operating at 760 Torr was pressure broadened. The sealed CO reference cell was filled at a total pressure of 150 Torr.

To verify the linear response of the mid-infrared QEPAS based CO sensor platform a calibration mixture of 5 ppm CO:N_2 was diluted with dry N_2 down to 50 ppb CO concentration levels and at each dilution step a constant 2.6% concentration of water vapor was added to the system (Fig. 7(a)). The data acquisition time for these measurements was set to 1 sec. The measured QEPAS signal amplitude as a function of CO concentration, are plotted in the Fig. 7(b). The calculated R-square value, which represents how well the regression line approximates real data points, is equal to ~0.999 after a linear fitting

#179896 - $15.00 USD Received 13 Nov 2012; revised 29 Dec 2012; accepted 29 Dec 2012; published 9 Jan 2013

procedure. This implies that the sensor system exhibits a good linearity response to monitored CO concentration levels. However, due to the decrease of the modulation depth to 0.26 cm^{-1}, the measured signal amplitude of moisturized 5 ppm CO:N_2 mixture is 22% lower compared to the line scanning mode experiments where a 0.325 cm^{-1} modulation depth was used. Based on the data in Fig. 7(a), the calculated MDL is 1.9 ppbv which is still in good agreement with the MDL value that was previously calculated for the QEPAS sensor operated in the scanning mode. The re-calculated NNEA coefficient in this case is 2.04×10^{-8} $cm^{-1}W/\sqrt{Hz}$.

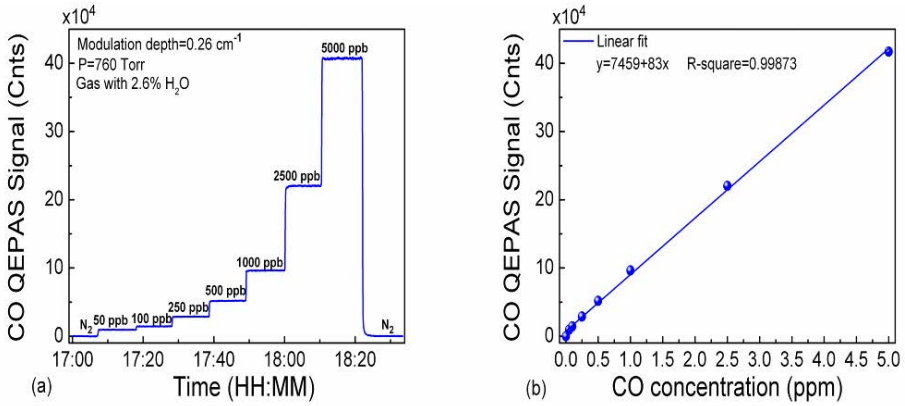

Fig. 7. (a) QEPAS signal amplitude recorded in the line locking mode as the CO concentration is varied at atmospheric pressure and a modulation depth of 0.26 cm^{-1}. (b) QEPAS signals amplitude averaged from Fig. 7(a) as a function of CO concentration. 1cnt = 6.67×10^{-16} A.

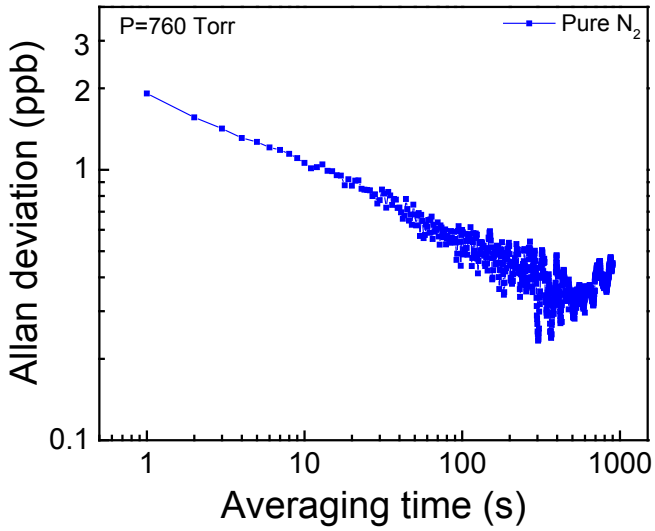

Fig. 8. Allan deviation plot for time series measurements of pure N_2 for the QEPAS based CO sensor system.

To investigate a long term stability and precision of the CO QEPAS sensor an Allan deviation analysis was performed when pure N_2 was passed through the sensor. From the Allan deviation plot shown in Fig. 8 the optimum averaging time for the CO sensor is found to be 500 sec, which results in a MDL of 340 pptv. A similar Allan deviation analysis was also performed for the N_2O QEPAS sensor when the laser wavelength was locked to the P(41) N_2O line. In this case, after averaging acquired data for 500 sec the MDL is improved to 4 ppbv. The reported N_2O detection limit of 4 ppbv at 500 sec averaging time is at least one

#179896 - $15.00 USD Received 13 Nov 2012; revised 29 Dec 2012; accepted 29 Dec 2012; published 9 Jan 2013

order of magnitude lower than previously reported in the literature when stronger N_2O absorption lines were selected [10–13]. This is not surprising because the non-optimum P(41) N_2O line has an absorption coefficients of ~60 times lower than any of the reported lines in Refs. [10–13]. However, using a similar QEPAS excitation power as available at the N_2O P(41) line and selecting for example N_2O R(14) line at 2235.49 cm^{-1} or N_2O R(18) line at 2238.36 cm^{-1} as discussed in Ref. [10], the MDL would be improved ~60 times reaching a level of ~0.07 ppb for an averaging time of 500 sec.

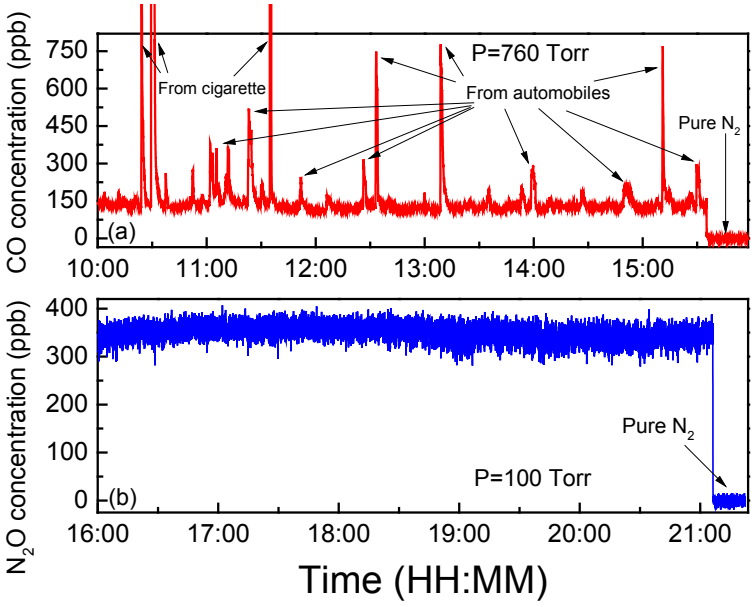

Fig. 9. Continuous monitoring of atmospheric CO and N_2O concentration levels from an air sampled on Rice University campus, Houston, TX, USA (Latitude and longitude are: 29° 43′ N/95° 23′ W). (a) CO concentration measurements; (b) N_2O concentration measurements.

For ambient CO and N_2O concentration measurements, an inlet tube of the QEPAS sensor was placed outside the laboratory and the atmospheric air was pumped into the sensor. The results of continuous measurements of atmospheric CO and N_2O concentration levels for a 5 hour period are shown in Fig. 9(a) and 9(b), respectively. The highest CO concentration spikes are caused by cigarette smoke when a smoking person breathe into the tube directly whereas all other less intense spikes, recorded on top of the CO atmospheric background of ~130 ppbv, are due to automobile emissions coming from traffic on Rice University campus road ~20 meters away from the sensor sampling inlet. The mean atmospheric concentration of N_2O was calculated to be 350 ppbv when using the P(41) N_2O line at 2169.6 cm^{-1}. Due to a long atmospheric residence time, the N_2O concentration is well mixed in the lower atmosphere and therefore its atmospheric concentration level is relatively stable as can be seen from Fig. 9(b).

4. Conclusions

A compact and interference free CO and N_2O QEPAS based sensor using the 4.61 μm high power CW TEC DFB-QCL operating at 10°C was demonstrated. The use of a high power CW DFB-QCL resulted in excellent CO detection sensitivity comparable to other more complex trace gas sensor platforms such as TDLAS with conventional multi-pass gas cell or cavity enhanced spectroscopy [30,31]. Wavelength modulation spectroscopy and a 2nd harmonic detection technique were used to reduce the sensor background noise and to achieve MDL values that are sufficient for environmental detection of CO and N_2O concentration

#179896 - $15.00 USD Received 13 Nov 2012; revised 29 Dec 2012; accepted 29 Dec 2012; published 9 Jan 2013

levels. Furthermore enhancement of the QEPAS signal can be realized by the addition of water vapor to improve the vibrational-translational relaxation rates of the two analyzed gas species. The experimental QEPAS system was tested in both scanning and line locking operational modes using acquisition time of 1 sec. For the CO sensor system operating in the line scanning mode at the atmospheric pressure, a 1.5 ppbv MDL at 2169.2 cm^{-1} was achieved when modulation depth was set to 0.325 cm^{-1}. The corresponding NNEA was calculated to be 1.61×10^{-8} $cm^{-1}W/\sqrt{Hz}$. In the line locking mode, due to a small reduction of modulation depth to 0.26 cm^{-1}, a MDL of 1.9 ppbv and obtained. For N_2O concentration measurements at 2169.6 cm^{-1} performed at an optimum gas pressure of 100 Torr, the MDL and NNEA were calculated to be 23 ppbv and 2.91×10^{-9} $cm^{-1}W/\sqrt{Hz}$, respectively. Furthermore, from the performed Allan deviation analysis the QEPAS sensor signal can be effectively averaged up to 500 sec. Environmental data averaged for 500 sec can significantly improve CO and N_2O MDL levels up to 340 pptv and 4 ppbv, respectively. The continuous monitoring of atmospheric CO and N_2O concentration levels for >5 hours indicated the stability and robustness of the reported DFB-QCL based QEPAS sensor system. The described CO and N_2O QEPAS-based optical sensor platform can be enclosed in an enclosure measuring 12 x 5 x 5 inches similar to a recently reported NO sensor in Ref. [32]. This sensor platform has a weight of ~4kg and is powered by CEU that requires ~50W of electrical power consumption. A fast sensor response time of <5 sec was obtained by using an ultra compact ADM and minimizing the length of the system tubes. With a detection sensitivity at single ppb concentration levels the reported CO and N_2O QEPAS based sensor is suitable for applications in environmental monitoring, atmospheric chemistry, industrial chemical analysis and medical and biomedical diagnostics as well as in law enforcement.

Acknowledgments

The Rice University group acknowledges financial support from a National Science Foundation (NSF) grant EEC-0540832 entitled “Mid-Infrared Technologies for Health and the Environment (MIRTHE)”, a NSF-ANR award for international collaboration in chemistry “Next generation of Compact Infrared Laser based Sensor for environmental monitoring (NexCILAS)” and the Robert Welch Foundation grant C-0586.

#179896 - $15.00 USD Received 13 Nov 2012; revised 29 Dec 2012; accepted 29 Dec 2012; published 9 Jan 2013